Available online at www.sciencedirect.com
SCIENCE DIRECT®
International Journal of Heat and Fluid Flow 25 (2004) 149–158
International Journal of HEAT AND FLUID FLOW
www.elsevier.com/locate/ijhff

Automated high-speed video analysis of the bubble dynamics in subcooled flow boiling

Reinhold Maurus *, Volodymyr Ilchenko, Thomas Sattelmayer

Lehrstuhl für Thermodynamik, Technische Universität München, 85747 Garching, Germany

Abstract

Subcooled flow boiling is a commonly applied technique for achieving efficient heat transfer. In the study, an experimental investigation in the nucleate boiling regime was performed for water circulating in a closed loop at atmospheric pressure. The test-section consists of a rectangular channel with a one side heated copper strip and a very good optical access. For the optical observation of the bubble behaviour the high-speed cinematography is used. Automated image processing and analysis algorithms developed by the authors were applied for a wide range of mass flow rates and heat fluxes in order to extract characteristic length and time scales of the bubbly layer during the boiling process. Using this methodology, a huge number of bubble cycles could be analysed. The structure of the developed algorithms for the detection of the bubble diameter, the bubble lifetime, the lifetime after the detachment process and the waiting time between two bubble cycles is described. Subsequently, the results from using these automated procedures are presented. A remarkable novelty is the presentation of all results as distribution functions. This is of physical importance because the commonly applied spatial and temporal averaging leads to a loss of information and, moreover, to an unjustified deterministic view of the boiling process, which exhibits in reality a very wide spread of bubble sizes and characteristic times. The results show that the mass flux dominates the temporal bubble behaviour. An increase of the liquid mass flux reveals a strong decrease of the bubble life- and waiting time. In contrast, the variation of the heat flux has a much smaller impact. It is shown in addition that the investigation of the bubble history using automated algorithms delivers novel information with respect to the bubble lift-off probability.

Keywords: Subcooled flow boiling; Bubble behaviour; Bubble life cycle; Automated high speed video analysis; Statistical results

1. Introduction

Nucleate boiling is a very efficient heat transfer mechanism and therefore applied in many technical applications. Traditional examples are steam generation in fossil and nuclear power plants, cooling of rocket burners and cooling of electronic devices. Besides these established fields also new applications appear at the horizon like e.g. two phase car engine cooling, which serve as the technical motivation for further research on boiling in the future. Subcooled boiling is characterised by the presence of small bubbles, which grow and collapse very rapidly on or near the heated surface. These bubbles are responsible for an extremely high augmentation of the heat transfer. Although a huge number of publications on the topic of boiling heat transfer exist, the basic knowledge of the physical mechanisms governing the boiling process is still incomplete although a big volume of data exists and models have been derived on a semi-empirical basis or highly simplified representation of the real processes. After all, the physics of boiling is contradictorily discussed and a full consensus has not yet been reached.

In the past, many investigations of the bubble behaviour and dynamics were performed. Due to the short time scale process, the bubble dynamic can only be resolved by the high-speed cinematography with frame rates above 1000 frames per second. The pioneering work of Gunther (1951) is well known. He was the first to study the bubble behaviour during subcooled flow boiling using the high-speed photography and quantified successfully the bubble size, the lifetime, the growth rate etc. as functions of system parameters like pressure, subcooling and velocity. Also Abdelmessih et al. (1972),

* Corresponding author. Tel.: 49-208-456-3824; fax: 49-208-456-2912.
E-mail address: reinhold.maurus@siemens.com (R. Maurus).

0142-727X/$ - see front matter © 2003 Elsevier Inc. All rights reserved.
doi:10.1016/j.ijheatfluidflow.2003.11.007

Nomenclature

d_B	bubble diameter (mm)	t_B	bubble lifetime (ms)
F_A	cumulative distribution function (–)	$t_{B,Abl}$	bubble lifetime after lift-off (ms)
G	liquid mass flux (kg/(m^2 s))	t_W	waiting time (ms)
N	number (–)	T	time (ms)
q	heat flux (MW/m^2)	W_B	probability (%)
ΔT_{Sub}	rate of subcooling (K)	X	coordinate streamwise (mm)
T_W	heater surface temperature (°C)	Y	coordinate transverse (mm)

Bibeau (1993), Kandlikar et al. (1995), Klausner et al. (1993) and others studied the bubble behaviour with optical high-speed techniques. Due to the lack of automated evaluation methods these researchers had to analyse the recorded films manually. Single bubbles were selected and tracked in the subsequent images of the high-speed film. [1] It is obvious that due to this laborious analysis technique the results of the bubble behaviour were mostly calculated from a very limited set of bubbles and experimental conditions. Despite the restricted width of the database, attempts were made to derive the behaviour of the "representative" bubble from the small fraction of information on the films exploited. An additional problem for the development of a common understanding of the boiling process is that some of the observed effects in different studies are not fully consistent. The experimental designs and the properties of the individual tests fluids are a major reason for these contradictory results. For example, the orientation of the heater surface to the gravitation field (horizontal or vertical) has a strong influence on the bubble detachment process, making a direct comparison very difficult.

The motivation for the investigation presented in the paper came from the fact that a statistical analysis of the bubble behaviour using a wide database was missing. Fortunately, the quick progress digital high-speed video techniques have made in recent years and the high-speed of modern computers in general allow the application of automated procedures for image processing in the future.

The main standard parameters characterising the bubble behaviour are the bubble size, the lifetime, which consists of the growth- and collapse time, the waiting time between two cycles and the bubble density on the heater surface. The aim of the presented work was the development of algorithms for an automated analysis of these bubble parameters in order to obtain a much wider database than available in the past.

[1] It is noted that Bibeau (1993) already started in this direction of bubble analysis by using some image processing and analysis algorithms to measure the size and the elongation of single bubbles.

2. Experimental setup

For the investigation of the bubble behaviour a test facility for flow boiling over a flat plate was built. The experimental facility was designed for water at low system pressure and the investigation of partially and fully developed subcooled flow boiling. Fig. 1 shows a sketch of the experimental setup. For a detailed description of the plant see Maurus et al. (2000).

The closed loop allows the variation of the operating pressure, the inlet temperature and the flow velocity. Using a variable speed pump, the liquid velocity through the test-section can be adjusted between 0 and 3 m/s. The minimum subcooling is limited to 5 K due to cavitation in the pump. A heat exchanger extracts the heat transferred to the flow in the test section. The fluid degassing tank in the by-pass of the loop removes non-condensable solved gases (mainly air) by heating the fluid up to the saturation temperature. The degassing process is started hours before and continues during the experiments.

Good optical access was an important aspect for the design of the test section (see Fig. 2). It is a horizontal rectangular channel of 500 mm length with a cross-sectional area of 40×40 mm^2. A nozzle upstream generates uniform inflow conditions. The copper bar having a wetted surface of 15 mm width and 200 mm length is

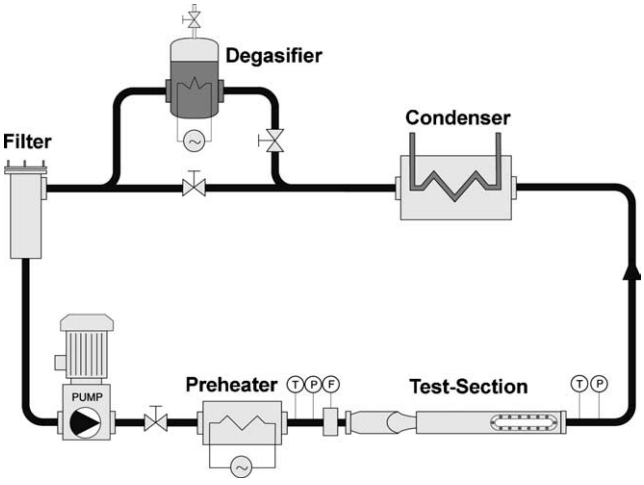

Fig. 1. Sketch of the test facility.

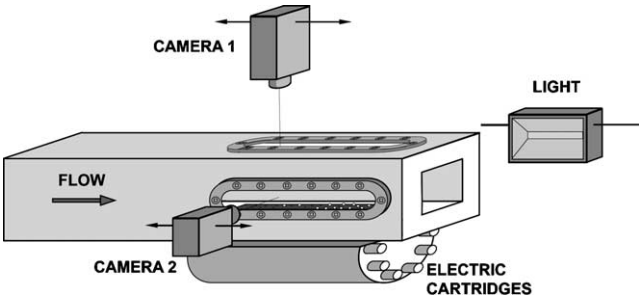

Fig. 2. Test-section and orientation of the camera to the heater surface.

heated with electric cartridges and provides a constant heat flux boundary condition, with a maximum of 1.50 MW/m^2. It is located in the middle of the lower wall. The heated surface starts 250 mm downstream of the entrance of the channel. Three observation windows allow optical access normal and parallel to the heated surface. The relatively small width of 15 mm results from a compromise between the desired two-dimensionality of the boiling process in the middle of the channel and the optical access to the central plane. All experiments were performed at steady state.

The optical arrangement is also sketched in Fig. 2. Two different cameras for the observation of the bubble behaviour are mounted on an optical bench. Camera 1 is a Sony XCD-900 with a relatively high resolution of 1280×960 pixels (8-bit) at a speed of 7.5 frames/s. The focal length of the receiving optics is 75 mm and the exposure time was 2 ms. The recorded sequence is limited to seven images. Already by using this camera and the view perpendicular to the heated surface, the bubble density and the void fraction could be measured (see Maurus et al., 2002). Camera 2 is a HS-Kodak Ektapro camera operated at a rate of 9000 frames/s with a resolution of 128×256 pixels. This speed delivers a sufficient temporal resolution (0.11 ms) of the observed boiling patterns. The focal length of the receiving optics is 105 mm. For each point of operation 1000 frames were recorded.

Simple backlighting was used in the high-speed video recordings. The advantage of this technique is the high light intensity, which is needed to obtain extremely short shutter times at the high frame rates employed. A tungsten lamp (500 W) and an optical diffuser plate mounted between lamp and test section generates the high intensity diffuse white light.

Since the position of both cameras can be varied in two directions by a mechanical traverse, the boiling process can be recorded stepwise from the beginning to the end of the heater. Depending on the selected optical magnification, the accessed observation area can be varied from 10 mm up to 100 mm. Consequently, the maximal spatial resolution is about 40 micrometers per pixel for the high-speed camera and about eight micrometers for the high resolution camera.

The images recorded by the high-speed camera show an area of 32 mm length in main flow direction. The left side of the images is located 10 mm downstream of the beginning of the heated surface.

3. Automated bubble analysis

3.1. Image pre-processing

Fig. 3 shows a typical image of the high-speed video film. Before the bubbles behaviour could be analysed with the image analysis algorithms developed by the authors a number of image pre-processing steps were applied in order to enhance the image quality. In the first step the horizontal position is adjusted and the image is cropped to the region of interest. Using several filters, which take the distribution of all grey pixel values into account, the contrast between the object and the background is enhanced and equilibrated. Morphological algorithms are applied and fill the bright bubble centres, which results from the light reflection and refraction at the bubble boundary. For a more detailed description of the procedures see Maurus et al. (2002).

As sketched in Fig. 4, the pre-processed images (X–Y plane) are stacked in their temporal sequence (T-axis), generating a three-dimensional array, which is the basis for the bubble analysis using the various subsequently described algorithms. The X-axis is here defined as the coordinate in downstream flow direction, the Y-axis as the coordinate normal to the flow direction. The T-axis results from the time period of the recorded high-speed film.

3.2. Functionality of the analysis algorithms

Fig. 5, which consists of the 30 reduced X–Y images of the 3D array, shows the temporal evolution of the bubble size. In the first 10 images (time steps) the rapid growth process can be seen. Between images 11 and 15

Fig. 3. Typical image of the high-speed video film.

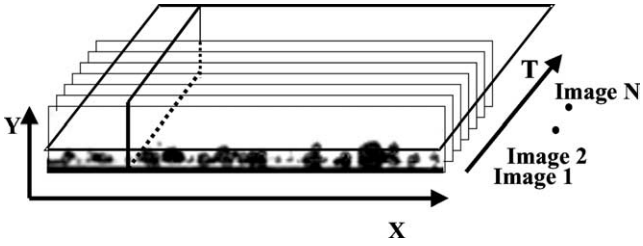

Fig. 4. Generating a three-dimensional X–Y–T matrix.

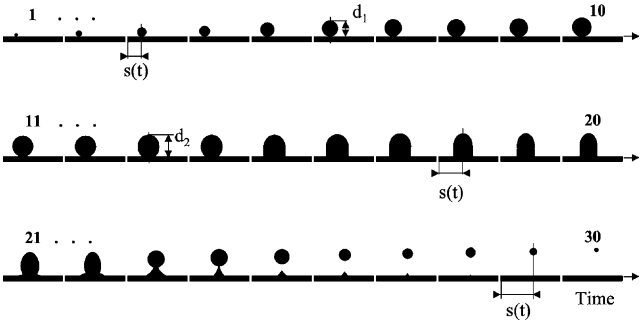

Fig. 5. Sequence of 30 reduced images showing the life cycle of a bubble.

the bubble form changes only slightly. After that, the bubble detachment process begins due to the buoyancy force. Finally, the bubble detaches from the surface and condenses rapidly due to the subcooled fluid in the outer region of the boundary layer. Note that after the bubble lift-off although most of the vapour is transported away from the surface, a small fraction remains on heated surface. Interestingly, the vapour attached to the wall condenses very rapidly due to the induced flow towards the surface. During the total lifetime the bubble is dragged in streamwise direction by the main flow. This is indicated by the value $s(t)$ in all reduced images of Fig. 5. The difference of this value at the bubble nucleation (first image in Fig. 5) and at the bubble condensation is the magnitude of the bubble motion along the heater surface during the total bubble lifetime.

In order to obtain a more condensed visualisation of the temporal bubble development, collapse and slip, the information inherent to the 30 single images in Fig. 5 can be reduced by extracting the location of the interfaces at the position of maximal bubble diameter from every image. These locations change during the lifetime of the bubble. Before bubble detachment, only one value is obtained whereas three values exist directly after bubble detachment. These are the maximum and the minimum distance of the bubble from the wall in wall normal direction and the position of the interface of the rest vapour remaining on the heater surface. All the important bubble data can be displayed as a function of time as shown in Fig. 6 for one single bubble. With this length and time scale diagram, for example, the bubble lifetime up to the detachment point or the rest lifetime of the bubble after lift-off is visualised and can be easily quantified by measuring the span on the horizontal axis, which now represents the time period of this occurrence. On the other hand the vertical axis represents the maximal bubble diameter at each time step. It can be seen, that the bubble growth rate drops with increasing bubble lifetime. By a more precise view of Fig. 6, it can be recognised, that the bubble diameter growth rate follows approximately a square root law, which was observed previously by other authors.

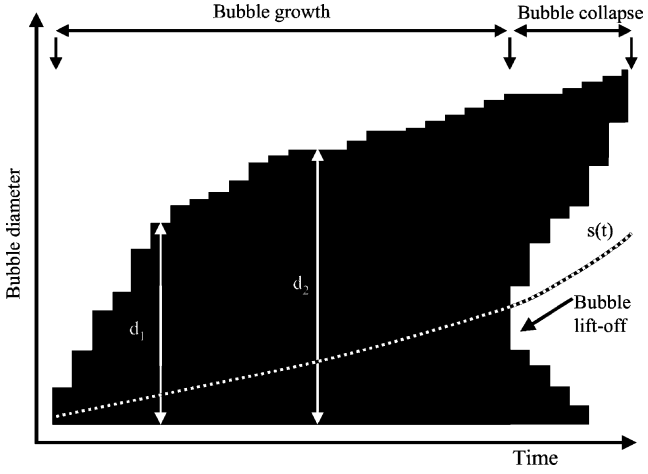

Fig. 6. Reduced view of the temporal development of the bubble diameter.

In the shown example the bubble detaches and collapses subsequently. The vapour sticking to the wall condenses as well. The time scale of both condensation processes is of the same order of magnitude. Additionally the relative motion of the bubbles along the heater is displayed in Fig. 6. Up to the bubble lift-off point the velocity of the motion is almost constant, but accelerated afterwards by leaving the near wall boundary layer and reaching spheres with higher fluid velocity. The total slip is in the order of the half maximal bubble diameter. Here it is noted, that the bubbles are assumed to have a spherical form. This assumption could be acknowledged by mounting the high-speed camera perpendicular, which allows a top view onto the heater surface. On the recorded films a realistic view of the bubble lifecycles was obtained. Further could be seen clearly, that for the investigated rate of subcooling ($T_{sub} = 10$–30 K), the bubble shape divers only marginally from a spherical form. In contrast, with further increasing fluid temperature ($T_{sub} < 10$ K), the bubble volume increases and also the shape differs more and more from a spherical form.

The algorithms to extract the interface curves in each image of the three-dimensional matrix are not too difficult and basically performed by gradient operations. In contrast the algorithms had to be refined for the reliable detection of all bubbles in the entire 3D array in order not to miss bubbles and not to analyse a bubble twice. Subsequently a brief description of the functionality of the developed algorithm is given, which routines were programmed in the high performance programming language MATLAB®. Due to those various included state-of-the-art image processing functions and analysis tools the effort for programming was tolerable.

After the generation of the 3D matrix presented in Fig. 4 a new two-dimensional X–T matrix is generated. In Fig. 7 this is shown in form of a table with zero and non-zero values. The non-zero values, which are strin-

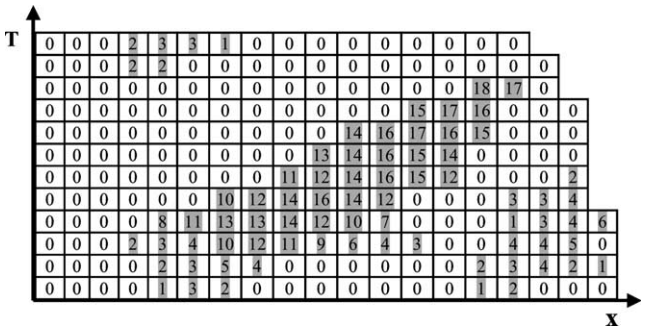

Fig. 7. Two-dimensional auxiliary matrix for successful realisation of the bubble tracking.

ged together, represent the heights of the bubble contour over the heating surface at the dedicated (x,t)-positions. If these values are smaller than or equal to the height of the heater surface, the values are set to zero. This means, that there exists no bubble at this time and position. Each string in the matrix, separated by the zero values, indicates the development of the bubble diameter. The maximum value in such a series defines the position and time step, where the bubble dimension is tallest. The task of the tracking algorithm is to trace the position of the maximal bubble diameter in all strings in temporal direction. After all these (x,t)-positions have been detected, the corresponding Y values are extracted from the 3D matrix along the total bubble lifetime to combine them in the way presented in Fig. 6. But in this case two issues become evident. First, the bubble slides during its growth period. Secondly, due to the finite depth of the focus, the real maximum can be lost, because another bubble out of focus can be involved in the routine by appearing in front of or behind the bubble under investigation. For this reason, a more sophisticated logical error analysis for the extracted sequences is required. This is performed by defining criteria, which are obtained empirically by intensive observation of the bubbles behavior in the recorded high-speed films. One criterion for the validation of a proper bubble evolution is the direction of the drift of the maximum. A drift in upstream direction is excluded, which makes physically no sense. Another criterion allows only a limited shift between two consecutive strings in streamwise direction. Similar to the drift the bubble growth rate (represented by the Y value) between two time steps is restricted. Finally, the extracted sequence along the bubble lifetime, as is shown in Fig. 6, must not have more than one maximum. Otherwise the probability is very high, that the investigated bubble has been lost and another out of focus bubble gets involved in the tracking routine. If only one of the mentioned criteria is fulfilled, the results of the investigated bubble are ignored in order not adulterate the statistical results. During the program operation, every investigated bubble has to be marked, in order not to analyse and count one bubble twice. This

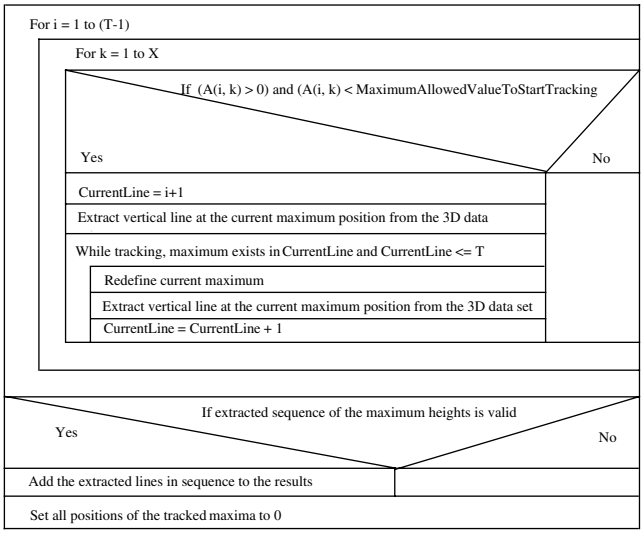

Fig. 8. Nassi–Shneiderman diagram.

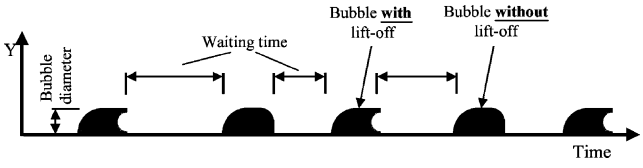

Fig. 9. Waiting time and bubble lift-off probability.

is performed by setting all values of the consecutive string, which belong to the actually investigated bubble cycle, to zero, after the bubble evaluation is completed. After the full application of these algorithms many "reduced images", each representing one bubble, are generated, as shown in Fig. 6. On this basis, the automated extraction can be visually controlled and afterwards all relevant parameters are straightforward for the statistical analysis. To summarise the full structure of the program Fig. 8 shows in a simplified form the so-called Nassi–Shneiderman diagram of the tracking routine kernel. In this diagram "A" denotes the mentioned auxiliary matrix of the interface curves.

Fig. 9 shows a result of another tracking routine applied for the whole 3D matrix. Because this algorithm is similar but more simple than the previously described routine, the functionality will not be explicated in detail in order not to go beyond the scope. Using this kind of X–T matrix, the waiting time between two bubble cycles [2] can be precisely quantified, by measuring the distance between two bubbles on the time axis. In addition, information about the bubble detachment behaviour can be extracted by analysing the shape of the bubble diameter in the Y–T plane. In the case of a bubble with detachment the pixel cluster shows a "C-shaped" right

[2] The bubble frequency ($=1$ / bubble waiting time) frequently used in the literature has an equivalent physical meaning.

side. Alternatively, the cluster has an almost semi-circle shape (see Fig. 9) as long as it does not detach from the wall. After many bubbles have been evaluated, the ratio of the occurrence of both shapes delivers the information concerning the lift-off probability.

4. Results and discussion

In the following graphs results extracted by means of the previously described automated algorithms are presented. In the experiments the liquid mass flow rate and the heat flux were varied keeping the rate of subcooling and the system pressure (atmospheric) constant. The heat flux was varied between 0.2 and 1.1 MW/m^2 and the mass flux was changed stepwise between 250 and 2000 kg/(m^2 s). The recorded high-speed films display an area of 32 mm length in main flow direction with the left side of the images located 10 mm downstream of the beginning of the heated surface. Due to the excessive number of analysed bubble cycles a statistical evaluation can be made.

The analysis of the data reveals a wide spread of the calculated values. For this reason, the usually applied averaging of these values to calculate a mean parameter should be avoided in order not to lose most of the information recorded during the experiments. [3] Subsequently instead of averaging, the results are presented in form of normal cumulative distribution functions. The horizontal axis shows the investigated physical parameter of the bubbles, which is also the allowable domain for the given probability function. Since the vertical axis with the parameter F_a represents a probability, it must fall between zero and one. It increases from zero to one as we go from left to right on the horizontal axis.

The uncertainty of the subsequent presented results is based on two reasons. Firstly, the temporal and the spatial resolution of the used camera is limited. In our case the time resolution, which depends on the frame rate, is 0.11 ms and the spatial resolution is around 0.13 mm. Specially for a very small bubble with short lifetime this limitation becomes more evident. Secondly, the errors of the functionality of the analysis algorithm have to be detected. This was performed by comparing the automated results with some manually analysed film sequences. It was ascertained, that for all comparisons both results agreed well within the range of 10%.

4.1. Bubble size distribution

The size distribution of the bubbles, shown in Fig. 10 for a constant heat flux and different mass fluxes, reveals

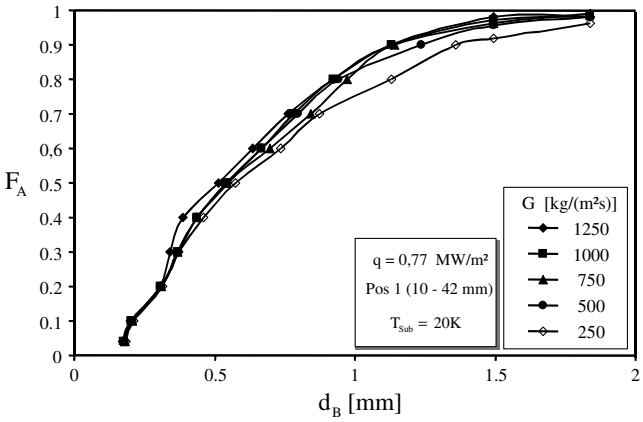

Fig. 10. Influence of the mass flux on the bubble size distribution.

that a huge number of small bubbles exist during the boiling process. Fifty percent of the observed bubbles have diameters smaller than 0.5 mm. Although the bubble density depends clearly on the liquid mass flux (Maurus et al., 2002), the bubble size distribution is only a very weak function of the main flow velocity. Increasing the mass flow by a factor of five leads to a very moderate decrease of the bubble size.

The bubble size distribution for a constant mass flux and different heat fluxes is depicted in Fig. 11. The high fraction of small bubbles becomes once more visible. An increase of the heat flux results in a slight increase of bubble size. Qualitatively, the same trends were observed for the mean bubble size by Abdelmessih et al. (1972) and Levy (1967), who studied the behaviour of selected bubbles in subcooled flow boiling of water at a vertically mounted stainless steel strip using high-speed photography.

4.2. Bubble lifetime

Fig. 12 shows the effect of the mass flux on the bubble lifetime, which includes the time difference between the

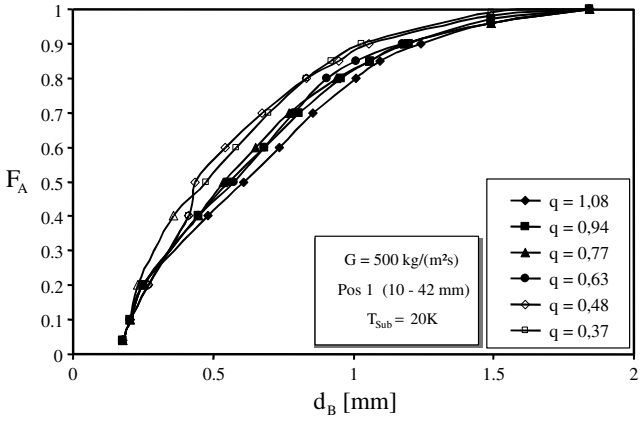

Fig. 11. Influence of the heat flux on the bubble size distribution.

[3] In the past, averaging was often applied to reduce scatter due to the low number of evaluated bubbles. This restriction could be overcome with the automated procedures developed by the authors.

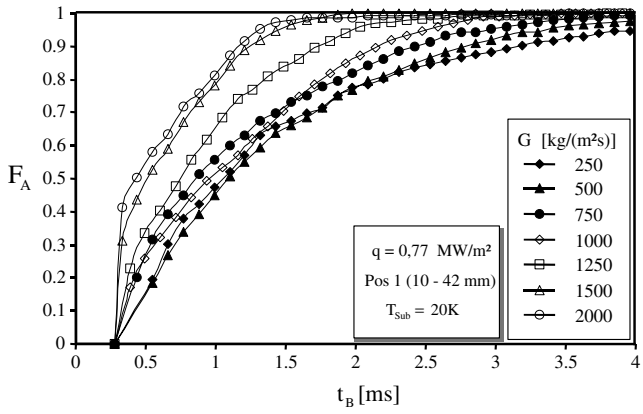

Fig. 12. Effect of the mass flux on the bubble lifetime.

nucleation process and the complete condensation, independent of the bubble lift-off behaviour. In comparison to the bubble size distribution the distribution functions have a remarkably similar form (see Figs. 10 and 11). The data evaluation reveals clearly that the very short lifetime of a high number of small bubbles is the physical reason behind this finding, which is consistent with the work of Bibeau (1993), who also detected a strong correlation of the bubble lifetime with the bubble size. With increasing mass flux the bubble lifetime decreases and it can be seen that for high mass fluxes ($G > 1500$ kg/(m^2 s)) no bubbles exceed a lifetime of 1,5 ms. The effect of the heat flux on the bubble lifetime is shown in Fig. 13. With increasing heat flux the distribution functions are also shifted towards higher lifetimes, but the effect is less dominant than the influence of the mass flux described previously.

The results of the liquid mass flux variation show good agreement with the findings of other authors like Gunther (1951), Zeitoun and Shoukri (1996) or Akiyama and Tachibana (1974), who also studied the bubble lifetime during subcooled flow boiling. The cause for the smaller size distribution is the reduced temperature in thermal boundary layer and the augmentation of turbulence with increasing mass flux. Both phenomena force the condensation at the bubble tip.

The effect of the heat flux on the bubble behaviour is discussed contrarily. Tolubinsky and Kostanchuk (1970) and Prodanovic (2001) determined no influence of the heat flux on the lifetime. According to Abdelmessih et al. (1972) the lifetime increases with heat flux, which is in good agreement with the findings of this study. In contrast Gunther (1951) observed a slight decrease of the lifetime with increasing heat flux.

4.3. Bubble lifetime after lift-off

Fig. 14 depicts the remaining lifetime of the bubbles after the lift-off from the heater surface. Similarly to the total lifetime the effect of the liquid mass flux is very dominant. Note that the remaining lifetime is roughly one order of magnitude smaller than the total lifetime. In Fig. 15 the influence of the heat flux is shown. Interestingly, the distribution functions are very similar

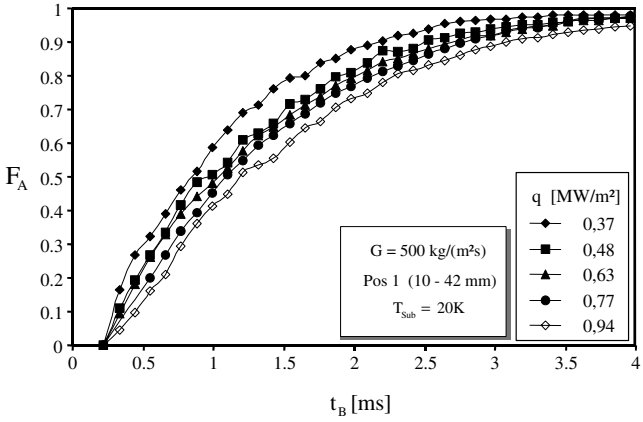

Fig. 13. Effect of the heat flux on the bubble lifetime.

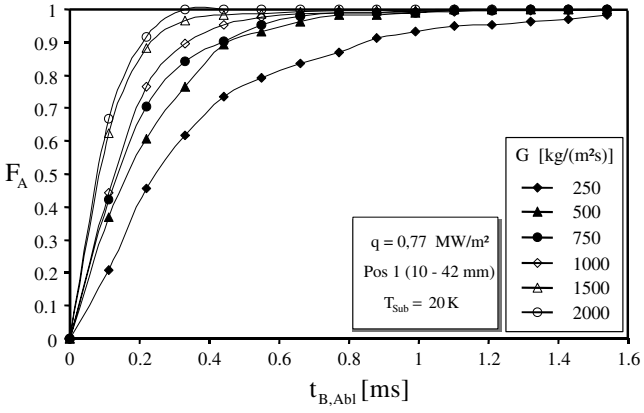

Fig. 14. Influence of the liquid mass flux on the rest lifetime after the bubble lift-off from the heater surface.

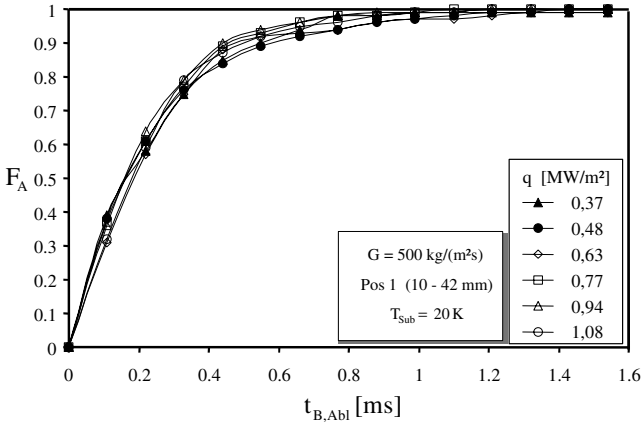

Fig. 15. Influence of the heat flux on the rest lifetime after the bubble lift-off from the heater surface.

revealing a vanishing influence of the heat flux on the remaining lifetime after lift-off.

The strong influence of the mass flux can be explained again by the increasing slip between both phases and the augmentation of turbulence in the liquid. The latent heat of the condensing vapour, which heats up the liquid near the bubble interface, is more effectively convected into the bulk liquid leading to a larger the temperature difference and condensation rate. This effect explains also the negligible influence of the heat fluxes at constant mass flux. Similar findings were described earlier by Lucic et al. (2003), who studied the heat transfer around single condensing bubbles in vertical subcooled flow boiling with holographic interferometry.

4.4. Waiting time between two bubble cycles

Fig. 16 shows the effect of the liquid mass flux on the waiting time between two bubble cycles. With increasing mass flux the waiting time is significantly reduced and shows a trend similar to the bubble lifetime. Fig. 17 depicts that the waiting time is not influenced much by increasing the heat flux. Only a slight reduction is observed.

The waiting time (respectively the bubble frequency) was frequently studied in the past. Ma (1998) performed measurements in horizontal and subcooled flows under normal as well as under reduced gravity. In both cases he observed a decrease of the waiting time with increasing mass flux. Abdelmessih et al. (1972) describe no influence of the mass flux on the waiting time but a clear trend for different heat fluxes, which is consistent with the data of the present study. In the experimental investigation made by Yin et al. (2000) in horizontal subcooled flow of refrigerant R134a a reduction of the waiting time with increasing heat flux as well with decreasing mass flux was found.

The established opinion concerning the effects leading to a well defined waiting time between two bubble cycles

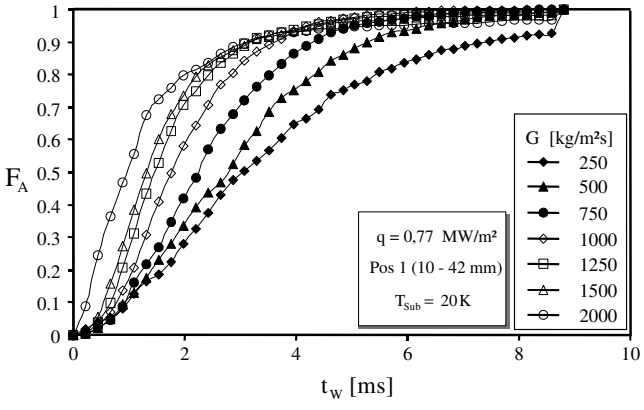

Fig. 16. Influence of the liquid mass flux on the waiting time between two bubble cycles.

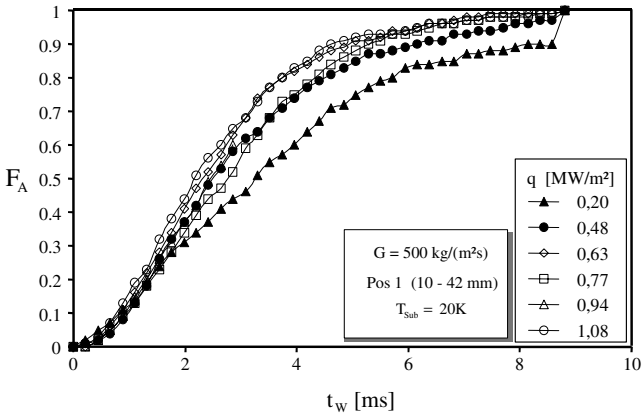

Fig. 17. Influence of the heat flux on the waiting time between two bubble cycles.

is as follows: During the bubble growth period a high rate of energy is extracted from the heater surface, which leads to a significant temperature drop. This decrease depends on the bubble size. Therefore the waiting time increases with the bubble size, which corresponds to the presented results. For a more extended explanation the bubble detachment process has to be observed more deeply. A short moment before detachment a ''bottleneck'' is formed between the bubble centre and the wall, which splits the bubble into two parts. The bigger vapour fraction is found in the sliding bubble, as shown previously, the remaining vapour condenses very rapidly. This leads to a strong fluid jet flooding the nucleating site. The site can be either flooded completely or partially depending on the fluid properties and the operating conditions. In case of complete flooding of the cavity a high superheat is required for the next bubble cycle. In case some vapour survives in the cavity, less superheat is required for the next nucleation to take place. The probability for an incomplete flooding of the size increases with the bubble diameter. On the other hand the amount of heat, which is extracted from the heater, increases with the bubble diameter. As the consequence, two parallel phenomena influencing the waiting time exist, which have the opposite effect. Depending on the system parameters and the fluid properties one of these effects dominates over the other. This interpretation of the reasons for the macroscopic findings corresponds to the results of Sultan and Judd (1978), who studied the influence of subcooling on the bubble waiting time. He observed that at low rate of subcooling (0–10 K) the waiting time decreases with subcooling and reaches a minimum at 10 K. For higher rates of subcooling the trend is reversed and the waiting time increases when subcooling is further increased. According to this interpretation, the presented results indicate a strong flooding of most of the nucleation sides during bubble condensation. As a consequence, it must

be expected that the heat conduction in the wall material determines the waiting time in our case.

4.5. Lift-off probability

Besides the results concerning the time scales of the boiling process, information about the detachment behaviour could be extracted by applying an analysis algorithms developed for this purpose. Fig. 18 shows the lift-off probability, which is indicated with the parameter W_B on the vertical axis, of the analysed bubbles for different mass- and heat fluxes. For all parameters the probability W_B lies between 20% and 65%. For small mass fluxes ($250 < G < 500$ kg/(m^2 s)) the fraction of bubbles, detaching from the surface, are independent of the mass flux. Increasing the mass flux the further leads to a drop of the lift-off probability.

Whether bubbles detach from the surface or not was contrarily discussed in the past. Del Valle and Kenning (1985) observed no bubble lift-off for horizontal subcooled flow boiling. In contrast, Bibeau (1993) and Thorncroft (1997) described that almost all studied bubbles detach during vertical subcooled flow boiling. These bubbles were carried away in streamwise direction until they condensed far away from their nucleation site. Obviously, the orientation of the gravitational field is crucial. The liquid drag and buoyancy are perpendicular for horizontal heater surfaces. In case of a vertical heater orientation both forces act in the same direction and foster bubble detachment. Bibeau postulated two different (normal and parallel) detachment modes. In the second case the bubbles slide along the vertical heater surface, while they still are in contact with the superheated boundary layer. Thus steam can evaporate into the bubbles while condensation takes place at the same time at the bubble tip (see also Thorncroft, 1997). By the normal detachment mode the bubbles are immediately ejected into the liquid core, where intense condensation takes place. If buoyancy acts perpendicular to the heater surface the detachment of a bubble is also followed by an immediate transport towards liquid core, which is similar to the normal detachment mode described by Bibeau (1993). In the present study the bubbles are exposed to a buoyancy force away from the heated surface. Consequently, very short lifetimes after the lift-off were measured.

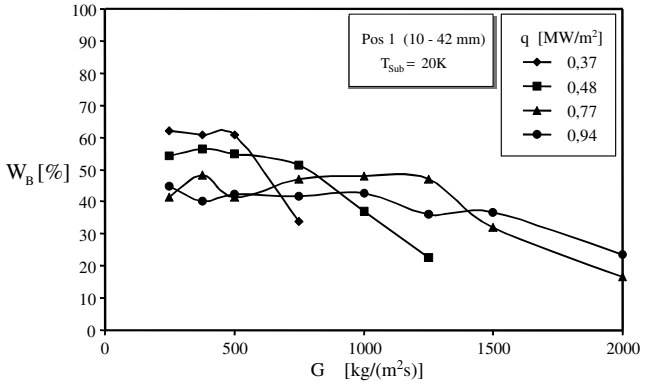

Fig. 18. Effect of the liquid mass flux and the heat flux on the bubble lift-off probability.

5. Conclusion

Boiling experiments in subcooled flow with a constant rate of subcooling and under atmospheric pressure conditions were carried out. The boiling process was visualised by a high-speed video technique. Using digital image processing and analysis algorithms an automated evaluation of the recorded high-speed films could be performed. From the results the following conclusion concerning the bubble behaviour can be drawn:

The bubble size distribution shows a high share of small bubbles. For small the bubble sizes, the distribution function depends only weakly on the heat flux and the liquid mass flux. However, the effects are more pronounced for bigger bubble sizes.

The total bubble lifetime, the remaining lifetime after the detachment process and the waiting time between two bubble cycles decrease significantly with increasing mass flux. The influence of the heat flux on this parameter is much weaker. The temperature of the thermal boundary layer and the turbulence intensity dominate the bubble behaviour, because both quantities govern the heat transport in the liquid near the interface.

The probability for bubble detachment varies for the selected experimental parameters between 20% and 65 % and depends on the mass and heat flux. For higher mass fluxes a lower fraction of the bubbles can detach from the heater surface.

Acknowledgements

The authors highly appreciate financial support by the Deutsche Forschungsgemeinschaft (DFG) in the frame of a Joint German Research Project on fundamentals of boiling heat transfer.

References

Abdelmessih, A.H., Hooper, F.C., Nangia, S., 1972. Flow effects on bubble growth and collapse in surface boiling. Int. J. Heat Mass Transfer 15, 115–125.

Akiyama, M., Tachibana, F., 1974. Motion of vapor bubbles in subcooled heated channel. Bull. JSME 17 (104).

Bibeau, E., 1993. Void Growth in Subcooled Flow Boiling For Circular and Finned Geometries for Low Values of Pressure and Velocity, Ph.D. Thesis, Univ. of British Columbia.

Del Valle, M.V., Kenning, D.B., 1985. Subcooled flow boiling at high heat flux. Int. J. Heat Mass Transfer 28, 1907–1920.

Gunther, F.C., 1951. Photographic study of surface-boiling heat transfer to water with forced convection. ASME Trans. 73, 115–123.

Kandlikar, S., Mizo, V., Cartwright, M., 1995. Investigation of bubble departure mechanism in subcooled flow boiling of water using high-speed photography. Convective Flow Boiling Conference, Banff, Canada, pp. 161–166.

Klausner, J.F., Mei, R., Bernhard, D.M., Zeng, L.Z., 1993. Vapor bubble departure in forced convective boiling. Int. J. Heat Mass Transfer 36 (3), 651–662.

Levy, S., 1967. Forced convection subcooled boiling-prediction of vapor volumetric fraction. Int. J. Heat Mass Transfer 10, 951–965.

Lucic, A., Emans, M., Mayinger, F., Zenger, C., 2003. Interferometric study and numerical simulation of the temperature field in the boundary layer and heat transfer in subcooled flow boiling. In: Proceedings of 5th International Conference on Boiling Heat Transfer, Jamaica.

Ma, Y., 1998. Forced Convection Boiling Heat Transfer in Terrestrial and Microgravity Environments, Ph.D. Thesis Washington State Univ.

Maurus, R., Hermanson, K.H., Sattelmayer, T., 2000. Measurements of the bubble behaviour and the phase boundary velocity in subcooled flow boiling. In: Proceedings of the 3rd European Thermal-Sciences Conference, vol. 2, pp. 719–724.

Maurus, R., Ilchenko, V., Sattelmayer, T., 2002. Study of the bubble characteristics and the local void fraction in subcooled flow boiling using digital imaging and analysing techniques. J. Exp. Thermal Fluid Sci. 26 (2–4), 147–155.

Prodanovic, V., 2001. Bubble Behaviour in Subcooled Flow Boiling at Low Pressures and Flow Rates, PhD Thesis Univ. of British Columbia.

Sultan, M., Judd, R.L., 1978. Spatial distribution of active sites and bubble flux density. Trans. ASME 100.

Thorncroft, G.E., 1997. Heat Transfer and Vapor Bubble Dynamics in Forced Convection Boiling, PhD Thesis, Univ. of Florida.

Tolubinsky, V.I., Kostanchuk, D.M., 1970. Vapour bubbles growth rate and heat transfer intensity at subcooled water boiling. In: 4th International Heat Transfer Conference, vol. 5.

Yin, C.-P., Yan, Y.-Y., Lin, T.-F., Yang, B.-C., 2000. Subcooled flow boiling heat transfer of R-134a and bubble characteristics in a horizontal annular duct. Int. J. Heat Mass Transfer 43, 1885–1896.

Zeitoun, O., Shoukri, M., 1996. Bubble behaviour and mean diameter in subcooled flow boiling. Trans. ASME J. Heat Transfer 118, 110–116.